Solvent Effects on Polysulfide Redox Kinetics and Ionic Conductivity in Lithium-Sulfur Batteries

Solvent Effects on Polysulfide Redox Kinetics and Ionic Conductivity in Lithium-Sulfur Batteries

Frank Y. Fan,[a,=,*] Menghsuan Sam Pan,[a,=,*] Kah Chun Lau,[b] Rajeev S. Assary,[c] William H. Woodford,[d,] Larry A. Curtiss,[c] W. Craig Carter,[a,**] and Yet-Ming Chiang[a,**,z]**

[a]*Department of Materials Science and Engineering, Massachusetts Institute of Technology, Cambridge, Massachusetts 02139, USA*
[b]*Department of Physics and Astronomy, California State University Northridge, Northridge, California 91330, USA*
[c]*Materials Science Division, Argonne National Laboratory, Argonne, Illinois 60439, USA*
[d]*24M Technologies, Cambridge, Massachusetts 02139, USA*

Lithium-sulfur (Li-S) batteries have high theoretical energy density and low raw materials cost compared to present lithium-ion batteries and are thus promising for use in electric transportation and other applications. A major obstacle for Li-S batteries is low rate capability, especially at the low electrolyte/sulfur (E/S) ratios required for high energy density. Herein, we investigate several potentially rate-limiting factors for Li-S batteries. We study the ionic conductivity of lithium polysulfide solutions of varying concentration and in different ether-based solvents and their exchange current density on glassy carbon working electrodes. We believe this is the first such investigation of exchange current density for lithium polysulfide in solution. Exchange current densities are measured using both electrochemical impedance spectroscopy and steady-state galvanostatic polarization. In the range of interest (1-8 M [S]), the ionic conductivity monotonically decreases with increasing sulfur concentration while exchange current density shows a more complicated relationship to sulfur concentration. The electrolyte solvent dramatically affects ionic conductivity and exchange current density. The measured ionic conductivities and exchange current densities are also used to interpret the overpotential and rate capability of polysulfide-nanocarbon suspensions; this analysis demonstrates that ionic conductivity is the rate-limiting property in the solution regime (i.e. between Li_2S_8 and Li_2S_4).

Manuscript submitted October 19, 2016; revised manuscript received November 10, 2016. Published November 25, 2016.

The widespread adoption of electric vehicles requires energy storage systems with higher energy density and lower cost than currently available batteries. The US Department of Energy's 2020 pack-level targets to enable widespread commercialization of electric vehicles are cost < \$125/kWh, energy density > 400 Wh/L, specific energy >250 Wh/kg, and specific power >2000 W/kg.[1] Sulfur is of interest as a cathode material for next-generation batteries because of its very low cost (as a by-product of oil and gas production, ~\$60 ton^{-1}) and high natural abundance. Moreover, its theoretical capacity of 1670 mAh/g as a lithium host (upon full reaction to Li_2S) is almost an order of magnitude higher than incumbent transition metal-based intercalation cathode active materials and may enable batteries with very high active materials-only theoretical specific energy (up to 2500 Wh/kg).[2,3] The low cost of active materials for the Li-S couple makes it an attractive option for large-scale grid energy storage applications as well, which are essential for the large-scale deployment of intermittent renewable energy sources such as wind and solar.[4]

Several technical barriers have limited the advancement of lithium-sulfur (Li-S) batteries, including rapid capacity fade, low rate capability, and low materials utilization.[5–9] During discharge of a Li-S cell, elemental S is initially reduced to form soluble polysulfide species Li_2S_x ($4 \leq x \leq 8$) which exist in complex solution-phase equilibria. Upon further discharge, the short chain polysulfides are further reduced and precipitate as Li_2S until the discharge end state is reached. These soluble polysulfide intermediates contribute to the rapid capacity fade of Li-S cells through the well-known shuttle effect, in which polysulfides diffuse toward and react with the lithium anode to form inactive insulating Li_2S on the lithium metal surface. The rate capability and materials utilization in a Li/S cell is affected by several factors, including the ionic conductivity of the electrolyte, exchange current density in the soluble regime (between Li_2S_8 and Li_2S_4), and nucleation and growth kinetics of the end-members, Li_2S and S. While numerous computational models have been developed for lithium-sulfur batteries, such models require independent experimental measurements of the fundamental transport and kinetic properties.[10–12] Previously, several of the present authors published an experimental study of the kinetics of Li_2S deposition from polysulfide solutions.[13] Here we extend our investigation to the important rate limiting processes in the soluble regime, where x in Li_2S_x is between 4 and 8, which have not been extensively reported.

We elucidate the rate-limiting transport properties of Li-S cells cycling through the soluble regime and demonstrate that solvent selection largely determines the bulk ionic conductivity and exchange current density, thereby influencing the rate capability of the Li-S cell. We present a systematic experimental investigation of ionic conductivity and exchange current density of lithium polysulfide solutions in ether-based organic solvents commonly used in lithium-sulfur batteries. Exchange current density was measured using electrochemical impedance spectroscopy and galvanostatic polarization. The measured transport properties were used to perform a critical analysis to determine the rate limiting kinetic mechanisms for Li-S cells of different configurations.

Especially important are the measurements of the sulfur concentration dependence of the transport and kinetic properties of lithium polysulfides. The electrolyte/sulfur ratio of a Li-S battery has a significant effect on its cost and energy density.[14] As sulfur dissolves into the electrolyte during discharge, the sulfur concentration and thus the properties of the electrolyte change. The electrolyte/sulfur ratio effectively sets an upper bound on polysulfide dilution. A cell with 20 ml electrolyte/g S, for instance, would have an upper bound on polysulfide concentration of approximately 1.6 mol S/L. On the other hand, if there is only 2 ml electrolyte/g S, total dissolution of sulfur would result in approximately 16 mol S/L, which exceeds the polysulfide solubility limit. Hence, we also investigated the effects of polysulfide concentration on exchange current density and ionic conductivity to understand the effects of high polysulfide concentrations that would occur in electrolyte-lean batteries. These concentration-dependent transport properties have remained poorly characterized to date; we anticipate that solution ionic conductivities will decrease with increasing sulfur concentration due to increased solution viscosity. Measurement and optimization of these transport properties is vital to the development of practical Li-S cells in the "lean" (low

=These authors contributed equally to this work.
*Electrochemical Society Student Member.
**Electrochemical Society Member.
zE-mail: ychiang@mit.edu

electrolyte/sulfur ratio) limit, where techno-economically viable cell designs are achievable.

Our experimental observations of solvent effects on exchange current density are in agreement with the results of first-principles simulations based on ab initio molecular dynamics (AIMD) simulations and static calculations.

Experimental

Preparation of polysulfide solutions.—To ensure the purity of lithium polysulfide solution, lithium sulfide (Alfa Aesar), sulfur (Alfa Aesar), and bis(trifluoromethane) sulfonimide lithium (LiTFSI, Sigma-Aldrich) were dried under vacuum overnight at 100°C. Solvents (Sigma-Aldrich) were dried for at least one week using molecular sieves. Li_2S_6 solutions were prepared with various sulfur concentrations (1–8 M [S]) and different organic solvents by mixing lithium sulfide and sulfur into the solvent in a 1:5 mole ratio. 0.5 M of LiTFSI salt was also dissolved into the solution as the supporting electrolyte. The tested solvents are tetra (ethylene glycol) dimethyl ether (tetraglyme), tri (ethylene glycol) dimethyl ether (triglyme), di (ethylene glycol) dimethyl ether (diglyme), and 1,3-dioxolane:1, 2 dimethoxyethane (DOL:DME 1:1). The resulting lithium polysulfide solutions were stirred overnight at 60°C to ensure homogeneity. Materials preparation, cell assembly, and exchange current density measurements were all performed in an Ar-filled glove box with oxygen and moisture levels below 1 ppm.

Exchange current density measurements.—Exchange current density experiments were performed using a 3-electrode setup with a 3 mm glassy carbon working electrode[15] (BioAnalytic Systems, Inc) and separate lithium metal electrodes (Alfa Aesar) as reference and counter electrodes. Deactivation of the glassy carbon surface was found to be the main source of error, which was minimized through consistent cleaning and preparation of electrode surfaces. The glassy carbon electrodes were polished using 0.3 μm and 0.05 μm alumina powder and stored under Ar to prevent surface contamination and used within 24 h of polishing.[16] In EIS experiments, sinusoidal voltages of 5 mV, 10 mV, and 15 mV amplitude were swept logarithmically from 10 kHz to 0.1 Hz between the working and counter electrodes. The three oscillation amplitudes were measured to verify linearity of the impedance response. The resulting impedance data (Fig. 1b) were fit to an equivalent circuit with the bulk resistance in series with a parallel configuration of the charge-transfer resistance and a capacitor (Fig. 1a). Exchange current density is then calculated from the fitted charge-transfer resistance R_{ct} according to Equation 1.

$$i_0 = \frac{RT}{zR_{ct}FA} \quad [1]$$

In the galvanostatic polarization experiments, a selected constant current was applied for 15 minutes to ensure steady-state conditions were achieved. The average electrode potential over each 15 minute step determined the corresponding potential for the applied current. After the 15 minute polarization, the cell relaxed under open-circuit conditions and then the experiment was repeated at a new applied current. Both oxidative and reductive currents were applied. Throughout the experiments, the solution was vigorously stirred to avoid mass-transport limitation. The current density-potential pairs from Figs. 2a and 2b were used to construct the Tafel plot for a given formulation; an example Tafel plot is shown in Fig. 2c. The linear region of the semi-logarithmic Tafel plot was manually fit and extrapolated back to zero overpotential to obtain the exchange current density according to the Butler-Volmer relation. All exchange current density measurements were performed using a Solartron 1470 potentiostat and 1455 Frequency Response Analyzer. The procedure for both EIS fitting and the Tafel extrapolation utilized Mathematica-based nonlinear least-square regression programs developed by our group.

Viscosity measurements.—The viscometric behavior of the different solutions was measured using a Malvern Kinexus Pro torsional rheometer enclosed in an Argon glove box with oxygen and moisture levels below 1 ppm. Steady shear viscometry tests were performed using a smooth stainless steel parallel plate geometry ($D = 40$ mm; mean roughness $Ra = 0.36$ μm). All tests were performed at $T = 25$°C and the temperature was regulated with a Peltier plate system. Steady shear tests were performed with decreasing applied shear rates. In addition, following the protocol proposed by Yoshimura and Prud'homme, the same sample was tested at three different gaps to probe and correct for slip effects.[17]

The flow curves of solutions containing 2.5, 5 and 7 M sulfur as Li_2S_8 in TEGDME with 0.5 M LiTFSI supporting electrolyte exhibited Newtonian liquid behavior with constant viscosity and no slip at the wall.

Ionic conductivity measurements.—Ionic conductivity of polysulfide solutions was measured using a Mettler Toledo FiveGo FG3 Portable Conductivity Meter calibrated with NIST-traceable aqueous solution standards. This measurement provides the total ionic conductivity of the solution.

Cell cycling.—Suspension electrodes were prepared from polysulfide solution (with 0.15 M $LiNO_3$ additive to reduce the effects of polysulfide shuttling) and carbon black (Ketjenblack EC-600JD), which were combined by manually stirring, followed by sonication for 1 h to form a percolating conductive network. This cathode architecture was used in order to access the solution regime directly without the need to undergo electrochemical sulfur dissolution. Cell cycling was performed in 2-electrode Swagelok cells controlled with a Bio-Logic VMP3 potentiostat. The suspension was placed inside a 0.5 mm well in a stainless steel rod current collector sputter-coated with gold. A porous polymer separator (Tonen) wetted with polysulfide-free electrolyte was used to separate the polysulfide positive electrode from the lithium foil negative electrode.

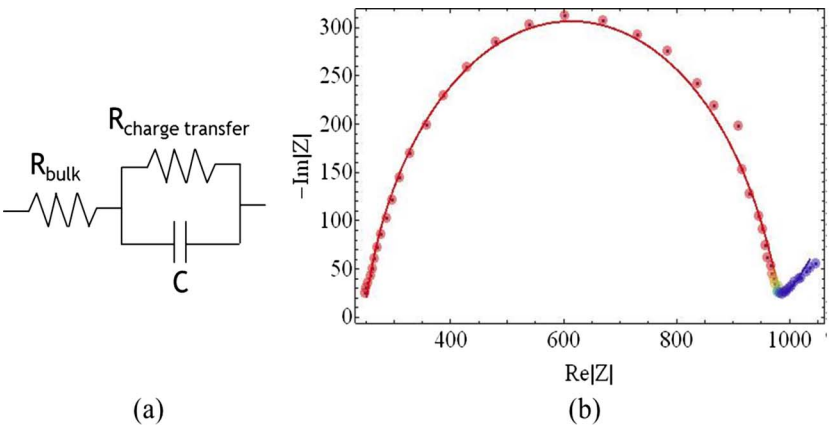

Figure 1. (a) Equivalent circuit for modeling the three electrode cell. The bulk resistance accounts for the ionic resistance while the charge transfer resistance describes the rate of reaction on the current collector surface. (b) Impedance response for polysulfide redox in diglyme solution. The charge transfer resistance and the exchange current density are calculated from the width of the arc.

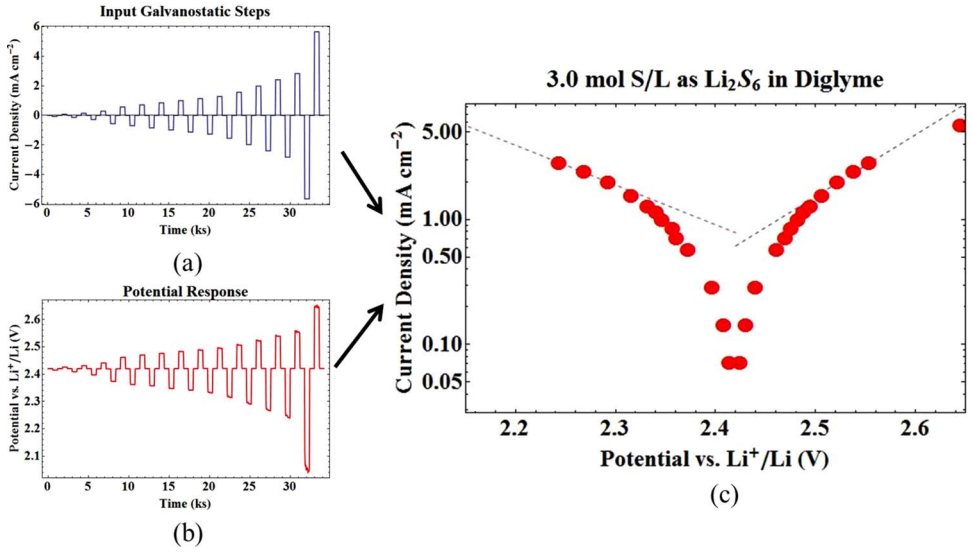

Figure 2. Galvanostatic polarization and resulting Tafel plot for 3.0 mol S/L Li_2S_6 in diglyme solution. The pairwise measured current step (a) and potential response (b) are used to obtain the Tafel plot (c). The semi-logarithmic linear regimes of the Tafel plots are extrapolated to the equilibrium potential to determine the exchange current density.

Calculation.—To compute the radial distribution function and coordination number of Li^+ for a solvated lithium polysulfide in various solvents, ab initio molecular dynamics calculations are performed using the VASP software.[18,19] All the calculations were spin-polarized and carried out using the gradient corrected exchange-correlation functional of PBE (Perdew, Burke, and Ernzerhof) under the projector augmented wave method, with plane wave basis set up to a kinetic energy cutoff of 300 eV.[20,21] The van der Waals method of Grimme, DFT-D2 was used throughout AIMD calculations with the convergence criterion of the total energy set to be within 1×10^{-4} eV.[22] To compromise with high computational cost, we only focus on one particular salt concentration (i.e. ~0.5 M LiTFSI) for these electrolytes (i.e. Diglyme, DOL:DME = 1:1, TEGDME, DME) with 2.5 M S-concentration throughout this work. For the simulation of different electrolytes (i.e. Diglyme, DOL:DME = 1:1, TEGDME, DME), the simulation box ($17.76 \times 17.76 \times 17.76$ Å^3) was randomly populated with 20–40 solvent molecules and 1 salt molecule (i.e., LiTFSI) with a solvated Li_2S_8 molecule with presumed liquid density of ~0.96 g cm^{-3}. To investigate the thermodynamic stability of the system at room temperature, all the system were thermally equilibrated at $T =$ 300 K based on an Nose–Hoover thermostat within NVT thermodynamic ensemble with a time step of 1 fs, and the production run (~3 ps) was obtained after thermal equilibration of ≈2.5 ps.

Static calculations using Gaussian 09 (Gaussian, Inc.) on model systems are also performed to compute the free energy of binding of lithium polysulfides (Li_2S_6 and Li_2S_8) with solvent molecules, and vertical electron affinity. The B3LYP/6-31+G* level of theory was used to compute the structure, electronic energy, vibrational frequencies, and free energy corrections of all species.

Results and Discussion

Exchange current density of polysulfide solutions.—Both electrochemical impedance spectroscopy and galvanostatic polarization are used because in a high volatility solvent system, the shift in sulfur concentration due to solvent evaporation may cause the exchange current density to change during the more time-consuming galvanostatic polarization measurement. More specifically, we have observed precipation in high concentration diglyme solutions as well as noticeable evaporation in DOL:DME 1:1 solutions after overnight exposure to Ar-filled environment. Thus, for these solvent systems, the EIS-based measurements are the most reliable. For the less volatile solvents, the measurements can be compared with each other. Our previous work demonstrated that there is good agreement between values obtained from these two methods, and both methods give similar results to steady-state voltammetry using an ultramicroelectrode.[23]

The dependence of exchange current density on both sulfur concentration and choice of solvent is shown in Fig. 3. Exchange current density increases linearly with concentration in diglyme through most of the concentration range tested, but has negative concavity in triglyme and tetraglyme. Tetraglyme, in particular, has roughly constant exchange current density at concentrations above about 4 M [S]. A positive correlation between concentration and exchange current density is to be expected because of the higher concentration of species available for reaction at the interface. However, the observation that exchange current density does not increase linearly with concentration shows that the rate constant for redox reactions decreases with increasing concentration. We believe that this effect is due to ion pairing at the very high concentrations found in our solutions, especially in triglyme and tetraglyme which have fewer solvent molecules per unit volume. Also, exchange current density may be limited by the number of active sites on the carbon surfaces.

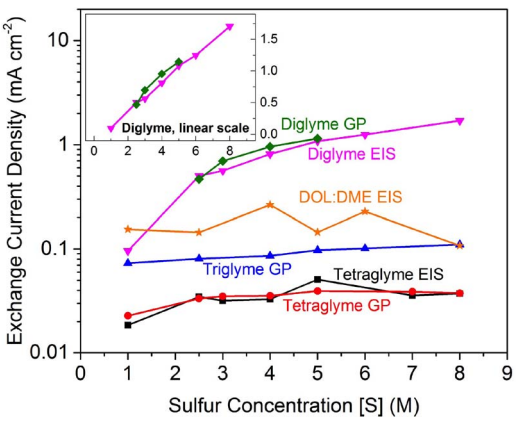

Figure 3. Exchange Current Density for Lithium Polysulfide (Li_2S_6) vs molar concentration of sulfur in difference ether-based solvent systems. Measurements for diglyme are also plotted in the inset to show the linear relationship between exchange current density and polysulfide concentration. Note: GP: Galvanostatic polarization, EIS: Electronic Impedance Spectroscopy

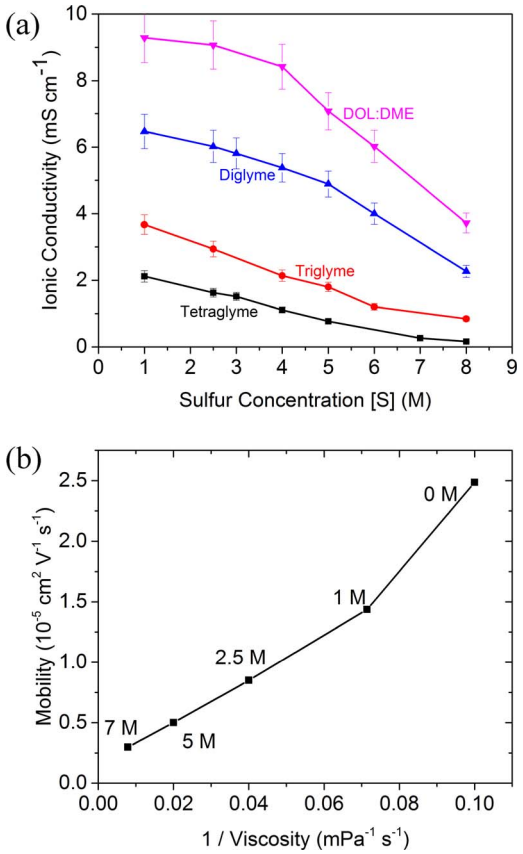

Figure 4. (a) Ionic conductivity of lithium polysulfide (Li_2S_6) vs. molar concentration of sulfur in different ether based solvent systems. All solutions contain 0.5 M LiTFSI as supporting electrolyte contributing to the total ionic conductivity. (b) Mobility of various polysulfide solutions in tetraglyme vs. inverse of viscosity, showing linear slope consistent with the Stokes-Einstein relation except for the "0 M" sample which contains supporting electrolyte salt and $LiNO_3$ additive, but no polysulfide.

In the pure ether solvent (tetraglyme, triglyme, and diglyme) systems, exchange current density increases as solvent molecule size decreases across all the concentrations measured. On the other hand, the DOL:DME 1:1 system has exchange current densities lower than that of diglyme even though DME molecules are smaller than diglyme molecules. The presence of DOL causes deviation from the molecular size trend because of the different functional group, which is expected to influence solvation of the active ions and polysulfide species. The solvation mechanism is discussed in detail in the computation section. In the four solvent systems investigated, the exchange current density increases by more than 15-fold from tetraglyme to diglyme. Thus, solvent selection may be expected to play a large role in the rate capability of Li-S cells.

Although this is a separate process from the nucleation and growth of Li_2S, we have previously found an improvement in nucleation and growth rates when switching from tetraglyme to diglyme of a similar magnitude to the exchange current density improvement described here, suggesting that these processes may be limited by similar mechanisms.[13]

Ionic conductivity of polysulfide solutions.—In the sulfur concentration range of interest (1–8 M of sulfur), ionic conductivity decreases monotonically with increasing sulfur concentration in all of the presently measured solvent systems (Fig. 4). This is consistent with observations of ionic conductivity in other solvent systems such as tetrahydrofuran.[24] For any given solvent, there are two opposing trends in ionic conductivity associated with increasing solute concentration: the number of ions available in the solution and the mobility of individual ions. The former increases with polysulfide concentration, but the viscosity also increases significantly with polysulfide concentration. Ion mobility is expected to decrease with increasing viscosity (Stokes-Einstein relationship). Here, the decrease in mobility apparently outweighs the increase in charge carrier density resulting from a higher concentration of lithium and polysulfide ions, resulting in an overall decrease in ionic conductivity. Figure 4b shows that the ionic conductivity of tetraglyme solutions varies linearly with inverse viscosity for all solutions except the "0 M" endmember which contains only salt and no polysulfide.

Note that the monotonic decrease of conductivity with polysulfide concentration may have significant implications for the performance of Li-S batteries with "lean" electrolyte/sulfur ratios. A low electrolyte/sulfur ratio increases polysulfide concentration in the electrolyte, and will reduce its ionic conductivity.

Comparing the ionic conductivity of the different solvent systems at any given sulfur concentration, the DOL:DME 1:1 system has the highest ionic conductivity, followed by diglyme, triglyme, and tetraglyme. All of the ethers used have the same functional group and differ only in the number of repeating units. The clear correlation is that ionic conductivity in the different solvents follows a trend of lower conductivity with longer solvent molecule. This finding is also consistent with the increasing viscosity with increasing ether chain length. At the higher polysulfide concentrations, the ionic conductivity is more than a factor of six higher for DOL:DME (1:1) than for tetraglyme. The ionic conductivity of Li_2S_8 measured earlier by our group also exhibits a similar trend with respect to sulfur concentration and solvent chain length as that of Li_2S_6 measured in this work.[25] We thus expect the ionic conductivity across different polysulfide species dissolved in non-aqueous solvents to follow the trend seen here. As with the exchange current density, the multifold variation in ionic conductivity across the solvent systems will impact rate capability, as shown next.

Cell capacity and rate capability.—To determine the effects of solvent on rate capability, cells using lithium polysulfide suspension (2.5 mol S/L) electrodes were cycled at C-rates of C/2, C, and 2C (Fig. 5). Cells using tetraglyme had the worst rate capability and the most polarization, as expected from the fact that tetraglyme has both the lowest ionic conductivity and lowest exchange current density. At a rate of C/2, the diglyme cell had the least polarization in the solution regime. However, at a rate of 2C, DOL:DME had lower polarization, which we attribute to ionic conductivity becoming the limiting factor at higher C rates. The tetraglyme cells also had high polarization in the precipitation regime, which is due to the relatively sluggish Li_2S electrodeposition kinetics compared to other solvent systems. Despite the relatively low conductivity and exchange current density observed for longer chain solvents like triglyme and tetraglyme, their significantly lower vapor pressure may make them useful for some applications, such as high-temperature operation or flow batteries.[23,26,27]

Calculation.—We found that diglyme binds to the lithium polysulfide species (Li_2S_6 or Li_2S_8) relatively weakly compared to triglyme and tetraglyme (see Figure 6 for computed structures). A likely reason is that there are only three oxygen atoms available for coordination with cations compared to triglyme or tetraglyme, which have four and five respectively. AIMD simulations are performed to demonstrate this hypothesis and understand the solvation environment. Simulations are performed for Li_2S_8 in TEGDME, Diglyme, DME and DOL:DME (1:1) solvent environments. For instance, based on the computed radial distribution analysis (rdf) and coordination number shown in Figure 7, a solvated Li_2S_8 species in diglyme has the lowest Li-O coordination number compared to DOL:DME (1:1) or TEGDME. The TEGDME solution has the highest Li-O coordination number in the first and second coordination shells. The assessment of radial distribution is confirmed by DFT calculations using cluster models. The computed Gibbs free energy of binding (298 K) of Li_2S_6 molecule with a clean glyme molecule in the gas phase is in the order: *TEGDME (−23.7 kcal/mol)> Triglyme (−22.2 kcal/mol)> Diglyme*

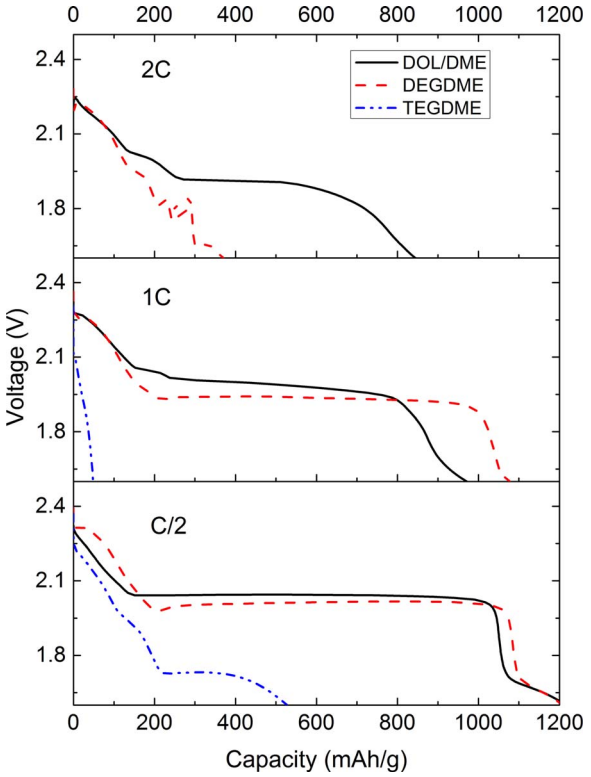

Figure 5. Voltage vs. capacity for first discharge of suspension-based Li-polysulfide cells at various C-rates using tetraglyme, diglyme, and DOL:DME (1:1). Tetraglyme results are not shown in the top panel.

(−12.2 kcal/mol). This trend is the same for Li_2S_8 species (Table I). Calculations are performed by including two diglyme molecules to provide an adequate number of oxygen atoms (four or more); however, the Gibbs free energy of binding (−12.5 kcal/mol) is similar, due to entropic contributions. Thus, computations suggest that the degrees of solvation of lithium polysulfides in various glymes are different. Relatively weaker binding of diglyme with the Li_2S_6 may allow the species to interact with other polysulfides that are in equilibrium or with the electrode surface. Since the exchange current densities reflect intrinsic rates of electron transfer between the lithium polysulfides and the electrode, we have computed the vertical electron affinity (EA_e) of the Li_2S_6:glyme complex (Table I) in the gas phase (B3LYP/6-31+G* level of theory) to provide a qualitative uunderstanding. They are in the order of: diglyme (+7.4 kcal/mol) > triglyme (+4.9 kcal/mol) > tetraglyme (+2.8 kcal/mol). This trend is consistent with the order observed in the measurement of exchange current density.

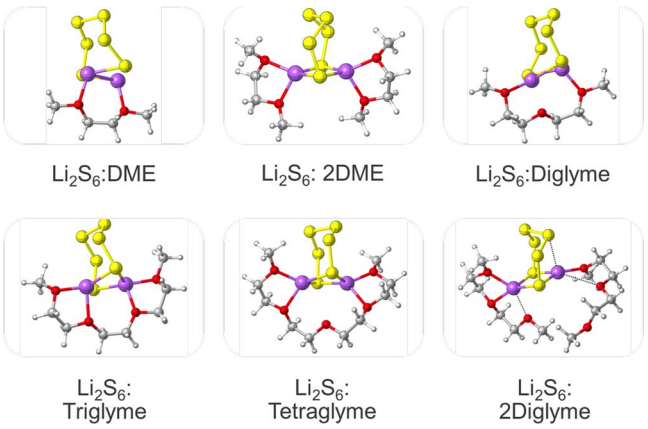

Figure 6. Optimized structures of selected Li_2S_6:Solvent complex computed at the B3LYP/6-31+G(d) level of theory.

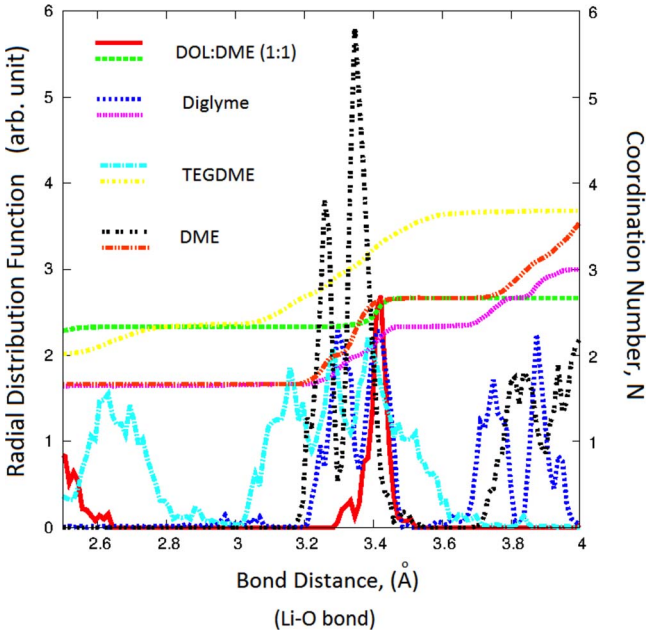

Figure 7. Computed radial distribution functions (RDF, top lines in legend) and coordination number (bottom lines) of solvated Li^+ from Li_2S_8 for bonds between Li^+ ions and O atoms in different solvent molecules from ab initio molecular dynamics (AIMD) simulations.

Table I. Computed gas phase free energies and enthalpies for the binding of Li_2S_6 with solvent molecules at the B3LYP/6-31+G* level of theory. (data associated with the Figure 1. Also shown is the computed Electron Affinity (EA) of the Li_2S_6-Solvent complex. Values in parenthesis are corresponding binding energies for Li_2S_8 molecule.

$(Solvent)_n$-Li_2S_6	ΔG (298 K)	ΔH (298 K)	EA of $(Solvent)_n$-Li_2S_6 (eV)
1-DME	−3.6	−16.2	−0.37
4-DOL	−4.2 (−4.7)	−47.5	
2-DOL:*1*-DME	−11.8	−45.2	−0.20
1-Diglyme	−12.2 (−13.6)	−26.5	−0.32
2-Diglyme	−12.5	−37.9	−0.18
2-DME	−17.3 (−18.4)	−38.9	−0.20
1-Triglyme	−22.2 (−22.6)	−38.6	−0.21
1-TEGDME	−23.7 (−21.3)	−41.9	−0.12

Conclusions

A systematic study of the effects of solvent choice and polysulfide concentration on exchange current density and ionic conductivity in lithium polysulfide solutions was performed for the first time. In any given solvent system, reaction rate constant and ionic conductivity are highest at low polysulfide concentrations, i.e. at high electrolyte/sulfur ratios. The choice of solvent significantly affects the kinetics and the rate capability of lithium-sulfur batteries. Within the glyme family of solvents, a decrease in the molecular weight of the solvent was found to increase significantly both exchange current density and ionic conductivity at a given polysulfide concentration. Significantly higher exchange current density was observed in diglyme than in the most

widely reported solvent system, DOL:DME. However, DOL:DME solutions had higher ionic conductivity than diglyme solutions. Although this resulted in lower polarization and higher rate capability for DOL:DME electrolytes in our test cells, other aspects of cell design, such as electrode thickness and the type and amount of conductive additive, will also play an important role in determining cycling performance. Diglyme may prove to be a superior choice under certain situations, such as when carbon surface area is limited and a higher exchange current density is beneficial, or where electrode thickness or tortuosity are low and ionic conductivity is less likely to be limiting. Tuning of kinetic parameters, ionic conductivity and exchange current density through careful electrolyte formulation design can significantly improve the rate capability of the lithium polysulfide solution, which is an important step toward realizing the potential low cost and high energy of the Li-S couple.

Acknowledgments

The authors thank Dr. Ahmed Helal for experimental assistance. This work was supported as part of the Joint Center for Energy Storage Research, an Energy Innovation Hub funded by the U. S. Department of Energy, Office of Science, Basic Energy Sciences.

References

1. D. T. Danielson, 1 (2014) http://energy.gov/sites/prod/files/2014/02/f8/eveverywhere_road_to_success.pdf.
2. S. B. Chikkannanavar, D. M. Bernardi, and L. Liu, *J. Power Sources*, **248**, 91 (2014).
3. P. G. Bruce, S. A. Freunberger, L. J. Hardwick, and J.-M. Tarascon, *Nat. Mater.*, **11**, 19 (2012).
4. B. Dunn, H. Kamath, and J. M. Tarascon, *Science (80-.).*, **334**, 928 (2011).
5. S.-E. Cheon et al., *J. Electrochem. Soc.*, **150**, A800 (2003).
6. A. Manthiram, Y. Fu, and Y.-S. Su, *Acc. Chem. Res.*, **46**, 1125 (2013).
7. G. Zheng et al., *Nano Lett.*, **13**, 1265 (2013).
8. R. Elazari et al., *J. Electrochem. Soc.*, **157**, A1131 (2010).
9. C. Barchasz, J.-C. Leprêtre, F. Alloin, and S. Patoux, *J. Power Sources*, **199**, 322 (2012).
10. A. F. Hofmann, D. N. Fronczek, and W. G. Bessler, *J. Power Sources*, **259**, 300 (2014).
11. D. N. Fronczek and W. G. Bessler, *J. Power Sources*, **244**, 183 (2013).
12. M. Marinescu, T. Zhang, and G. J. Offer, *Phys. Chem. Chem. Phys.*, **18**, 584 (2016).
13. F. Y. Fan, W. C. Carter, and Y.-M. Chiang, *Adv. Mater.*, **27**, 5203 (2015).
14. D. Eroglu, K. R. Zavadil, and K. G. Gallagher, *J. Electrochem. Soc.*, **162**, A982 (2015).
15. A. Dekanski, J. Stevanović, R. Stevanović, B. Ž. Nikolić, and V. M. Jovanović, *Carbon N. Y.*, **39**, 1195 (2001).
16. I. Hu, D. H. Karweik, and T. Kuwana, *J. Electroanal. Chem.*, **188**, 59 (1985).
17. A. N. N. Yoshimura and R. K. Prud'Homme, *J. Nonnewton. Fluid Mech.*, **32**, 53 (1988).
18. G. Kresse and D. Joubert, *Phys. Rev. B*, **59**, 1758 (1999).
19. G. Kresse and J. Furthmüller, *Comput. Mater. Sci.*, **6**, 15 (1996).
20. J. P. Perdew, K. Burke, and M. Ernzerhof, *Phys. Rev. Lett.*, **77**, 3865 (1996).
21. P. E. Blöchl, *Phys. Rev. B*, **50**, 17953 (1994).
22. S. Grimme, *J. Comput. Chem.*, **27**, 1787 (2006).
23. F. Y. Fan et al., *Nano Lett.*, **14**, 2210 (2014).
24. H. Yamin and E. Peled, *J. Power Sources*, **9**, 281 (1983).
25. W. Woodford et al., in *Meeting Abstracts*, p. 573, The Electrochemical Society (2014).
26. Y. Yang, G. Zheng, and Y. Cui, *Energy Environ. Sci.*, **6**, 1552 (2013).
27. X. Chen et al., *Energy Environ. Sci.*, **9**, 1 (2016).